

# Entanglement between Two Distant Observables of Quantum Current as the Mechanism of Radiation

Jeong-Wan Park(박정완)\*

Department of Physics and Astronomy, University of Hawaii at Manoa, Honolulu, Hawaii

(Dated: August 11, 2016)

In this paper, it will be demonstrated that entanglement between two distant observables of quantum electron current enables electromagnetic radiation of free-electron lasers even though the amplified quadrature and the radiated quadrature are out of phase. This is supported by the previously observed sub-Poisson photon intensity fluctuations in the coherent spontaneous harmonic radiation generated by an infrared free-electron laser.

*Introduction.*—Study of the quantized electromagnetic fields has been critical to the development of quantum optics. A classical electromagnetic field is described by a minimum uncertainty quantum state, i.e. the displaced vacuum state called a coherent state whose photon number fluctuations exhibit a Poisson distribution. Therefore, if the field of a free-electron laser (FEL) is a classical electromagnetic field, its photon number fluctuations should be a Poisson distribution. However Becker *et al.* analyzed the radiation of FELs in a fully quantized theory which is treating electron as a quanta of charged particle, and revealed the possibility that the photon number fluctuations of the FEL's fundamental component of the optical field can exhibit a sub-Poisson distribution[1].

To test their prediction, it was desirable to measure the photon number fluctuations of the FEL's fundamental component of the optical field[2]. However, the detector's quantum efficiency for that mode is low, whereas that for the 7th coherent spontaneous harmonic radiation (CSHR) of infrared (IR) FEL is higher[2]. (The fundamental component of the optical field creates the electron microbunching containing the discrete Fourier components of the electron current and enhances radiation of higher harmonics of the fundamental[2]). Thus, the photon number fluctuations of the 7th harmonic was measured in Chen's experiment which revealed a sub-Poisson distribution from the MARKIII FEL approaching saturation in the small signal regime, which neither confirmed nor contradicted the anticipation of Becker *et al.* for the fundamental mode[2]. This was the first experimental demonstration of a non-classical state of a radiation field created by a FEL[2]. The operation parameters used in the experiment are summarized in Table II.

The observed non-classical state cannot be created by classical electron currents or described by the deterministic electromagnetic field on which the classical analysis of the FEL operation based[2]. There have been attempts to explain the observed non-classical state using a shot-noise model which considers fluctuations of the radiating electrons' number density, or a quasi-classical model which treats the electron current classically and electromagnetic field quantum mechanically, but none of them were successful and quantum electron current was

strongly raised as a possible origin of the observation[3]. After these attempts, Madey pointed out that the observation could be explained by the velocity-dependent amplification of the component of vacuum fluctuations in quadrature with the acceleration-dependent radiation emitted by the electron microbunch[4].

In the research reported below, Chen's experimental data will be verified theoretically based on Madey's argument of vacuum fluctuations. His argument is based on the idea that vacuum fluctuations are related to the detection of photons, which is different from the common opinion in the quantum optics community as mentioned in [5].

Drawing this verification, it is found that the electrons' current density,  $J$ , should be treated as a quantum operator containing the quanta of photons. Furthermore, it is also found that entanglement between the two distant observables of the quantum  $J$  enables electromagnetic radiation although the radiated and the amplified quadratures are out of phase (a radiating deterministic electron cannot amplify field, but to radiate, it also needs to deliver the energy to field), which leads to the deduction that at the right edge of the wiggler (alternating magnetic field from the magnets in FEL) this entanglement cannot work, resulting in the sub-Poisson distribution of the observed photon number fluctuations.

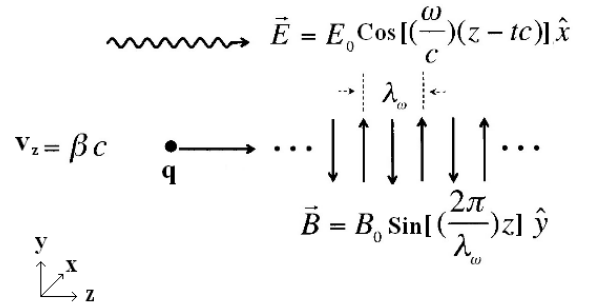


FIG. 1. Electron bunch in FEL's wiggler with co-propagating field.

*Two quadratures of FEL.*—To apply Madey's argument of vacuum fluctuations to FELs, we first need to identify the vacuum fluctuations' two quadratures for the

FEL field, which was firstly done in [6]. Consider the interaction of pre-formed electron bunches moving through a magnetic undulator with a co-propagating electromagnetic wave as shown in Fig.1. The co-propagating electric field proceeds to the positive  $z$  axis and the wiggler's periodic magnetic field is along the  $y$  axis. Then the electric field on the moving bunch treated as a point particle is

$$\vec{E} = E_0 \cos\left(\frac{2\pi}{\lambda_w} z + \Phi\right) \hat{x} \quad (1)$$

where  $\omega$  for the fundamental mode was chosen so that  $\frac{1}{2\gamma^2} \frac{\omega}{c} = \frac{2\pi}{\lambda_w}$ .  $\frac{\Phi}{\omega}$  is the time the bunch enters the undulator at  $z = 0$  and  $\lambda_w$  is the wavelength of the wiggler. Considering the bunch's Lorentz force due to the wiggler's magnetic field, we can obtain the amplified and the radiated field as the following:

$$\vec{E}_{amp} \propto -q\dot{x} \propto -q \int \ddot{x} dt \propto -\cos\left(\frac{2\pi}{\lambda_w} z\right) \quad (2)$$

$$\vec{E}_{rad} \propto q\ddot{x} \propto -\sin\left(\frac{2\pi}{\lambda_w} z\right) \quad (3)$$

As  $\Phi = \frac{\pi}{2}$  for the radiated field and  $\Phi = \pi$  for the amplified field in Eqn.(1), there is a  $\frac{\pi}{2}$  phase difference between the amplified and the radiated quadratures for FELs. For the vacuum fluctuations, there are two quadratures which have phase difference of  $\frac{\pi}{2}$ . Therefore, the above radiated and amplified field can constitute the two quadratures of vacuum fluctuations of FEL field.

*Squeezing of vacuum fluctuations and gain.*—We identify the two quadratures demonstrated above as follows.  $X_1$  is in phase with the emitted radiation (in phase with the electron's transverse acceleration) and  $X_2$  is in phase with the amplified field (in phase with the electron's transverse velocity). Assuming the FEL field for the 7th harmonic is a minimum uncertainty state, based on the claim that the fundamental mode is a minimum uncertainty[1], the uncertainty product of the two quadratures for the 7th harmonic will be constant though the individual ones can vary. Therefore, the uncertainty area is the same for (a), (b) and (c) in Fig.2.

To relate the FEL's two quadratures with the detected photon number's sub-Poisson fluctuations, recall the argument of Bachor and Ralph[4], which states that the amplification of the randomly fluctuating vacuum quadrature responsible for phase fluctuations reduces the amplitude of quadrature responsible for amplitude fluctuations, generating the amplitude squeezing state[7]. For the FEL field, as the electron can amplify  $X_2$  which is in phase with the transverse velocity, there would be a means to amplify  $X_2$  and measure the photon number. Then the FEL field will also be subject to amplitude squeezing, as the photon number count is along the  $X_1$  quadrature; the uncertainty ellipse on the  $X_1, X_2$  phase diagram for the radiated FEL field is centered on the  $X_1$

axis with a nonzero  $X_1$  value as (c) in Fig.2. The presence of this Squeezing Mechanism will be verified later.

When the Squeezing Mechanism is present, we can relate it with the gain of the FEL. Let the input quantum

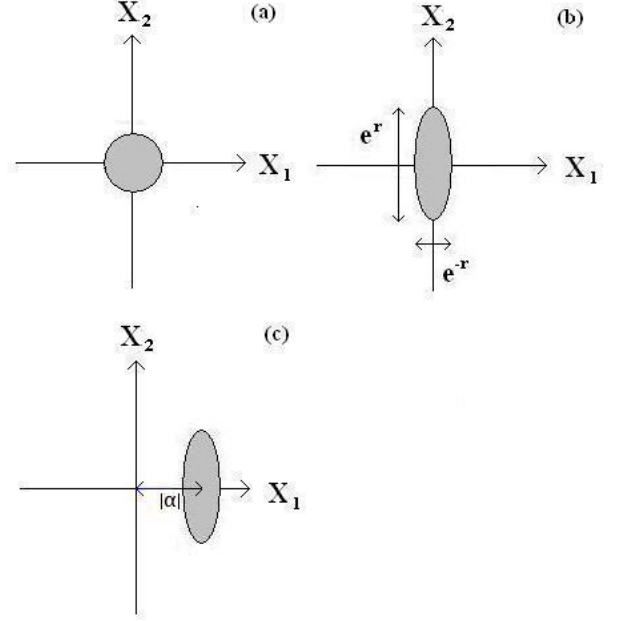


FIG. 2. Phasor diagrams: (a) Coherent vacuum state, (b) Minimum uncertainty squeezed vacuum state, (c) Squeezed state with nonzero  $|\alpha|$ , the radiated state. (c) has same uncertainty distribution as (b). The axes are normalized to have uncertainty area equals to one in this figure.

operator  $a_{in}$  for the 7th harmonic's vacuum fluctuations, before the influence of the Squeezing Mechanism, be

$$a_{in} = \frac{1}{2}(X_1 + iX_2) \quad (4)$$

And  $t_r$  is the time period when the Squeezing Mechanism is in effect. Then the output operator  $a_{out}$  for the vacuum fluctuations after  $t_r$  should be

$$a_{out} = \frac{1}{2}(\sqrt{F}X_1 + i\frac{1}{\sqrt{F}}X_2) \quad (5)$$

to keep the same magnitude of vacuum fluctuations' uncertainty area, where  $F < 1$  is the Fano factor of the output photon number's statistics.

Electrons can increase the 7th harmonic in two ways. The first is to increase  $\alpha$  along the  $X_1$  axis, which is the usual Radiation Mechanism. The second is to increase energy through squeezing vacuum fluctuations, such as the Squeezing Mechanism mentioned above. The gain  $G$  between time  $t$  and zero is

$$G = \Delta n = \frac{W(t) - W(0)}{\hbar\omega_7} = |\alpha|^2 + \sinh^2(r) = G_r + G_s \quad (6)$$

where  $W$  is the energy of the FEL field and  $G_s = \sinh^2(r)$ .  $r$  is defined in Fig.2 and  $\Delta n$  is the photon number from the above two mechanisms[8]. Here, the initial energy is zero. For a large  $|\alpha|^2$ , as in the case of [2] and a high gain in a higher harmonics as demonstrated in [9], the Fano factor becomes  $F \simeq e^{-2r}$ . Therefore, from Eqn.(6), we get

$$F = e^{-2r} = 1 + 2G_s - \sqrt{4G_s^2 + 4G_s} \quad (7)$$

*Classical gain calculation.*—To calculate the photon count rate and the Fano factor that will be compared to Chen's data, using Eqn.(6) and Eqn.(7), we need to calculate the gain of the 7th harmonic. First, define the phase of the fundamental mode,  $\xi = (k_w + k_1)z - \omega_1 t \simeq k_1 z - \omega_1 t$ .  $k_1, \omega_1$  are the wave number and angular frequency of the fundamental mode and  $k_w = \frac{2\pi}{\lambda_w}$ . The phase velocity is  $\nu = \frac{d\xi}{d\tau}$ , where  $\tau = \frac{ct}{L_w}$  which varies from 0 to 1, and  $L_w$  is the length of the wiggler. Then from

$$\frac{dc_m^n}{dt} = -\frac{1}{\epsilon_0 V_{opt_n}} \int d^3r \vec{J}_\perp \cdot \hat{x} e^{-in(k_1 z - \omega_1 t)} U_m^*(R, z) \quad (8)$$

we can obtain the  $c_m^n$ , the coefficient of the  $m$ th transverse cavity mode for the  $n$ th harmonic[3]. Here, approximate the lifetime of the 7th harmonic is infinite, which is proportional to the quality factor[10], and the current and fields are treated classically.  $U_m$  is the transverse mode and  $V_{opt_n} = \pi w_{0_n}^2 L_c$  is the volume of the cavity where  $w_{0_n}$  is the waist spot size of the  $n$ th harmonic and  $L_c$  is the cavity length, and

$$U_m(\rho, \zeta) = \sqrt{\frac{2}{1+\zeta^2}} L_m\left(\frac{2\rho^2}{1+\zeta^2}\right) e^{-\frac{\rho^2}{1+\zeta^2}} e^{i\Psi_m(\rho, \zeta)} \quad (9)$$

$$\Psi_m(\rho, \zeta) = \frac{\zeta\rho^2}{1+\zeta^2} - (2m+1)\tan^{-1}\zeta$$

where  $L_m$  is the  $m$ th Laguerre polynomial with  $\rho = \frac{R}{w_{0_n}}$  and  $\zeta = \frac{z - \frac{L_w}{2}}{z_R}$ .  $z_R$  is the Raleigh range and  $z$  is measured from the entrance of the wiggler and  $R$  is the transverse radius.  $z_R$  is related to  $w_{0_n}$  by  $z_R = \frac{k_n w_{0_n}^2}{2}$  where  $k_n = nk_1$ , and  $n$  is the harmonic number. Focus only on the lowest order transverse mode for the 7th harmonic's,  $c_0^7$ , then with  $c_0^7(0) = 0$ , Eqn.(8) becomes

$$c_0^7(t') = -\frac{J_0 J J_7}{\epsilon_0 V_{opt_7}} \int_0^{t'} \sum_{p=1}^{N_{\text{phase}}} \sum_{p_n=1}^{N(\xi_p, t)} \sqrt{\frac{2}{1+\zeta_{p_n}^2}} e^{-\frac{\rho_{p_n}^2}{1+\zeta_{p_n}^2}} e^{-(\frac{\zeta_{p_n} \rho_{p_n}^2}{1+\zeta_{p_n}^2} - \tan^{-1}\zeta_{p_n})i} e^{-7\xi_{p_n} i} dt \quad (10)$$

where  $J_0 = \frac{ecK}{2\gamma} \simeq 3.23 \times 10^{-13} [\frac{C \cdot m}{s}]$  and  $J J_7 = (-1)^{\frac{7-1}{2}} [J_{\frac{7-1}{2}}(7\eta) - J_{\frac{7+1}{2}}(7\eta)] \simeq -4.14 \times 10^{-2}$  with  $\eta = \frac{K^2}{4(1+\frac{K^2}{2})} \simeq 0.20$ .

In Eqn.(10), we can see the integrand will be significant only when the  $N(\xi_p, t)$  contains the large 7th component proportional to  $e^{7\xi_{p_n} i}$ ,  $\tilde{N}_7$ , considering the small variation of  $U_0^*$  compared to  $e^{7\xi_{p_n} i}$  within the electrons. When the electron beam enters the wiggler, assume the electrons of a microbunch are uniformly distributed in  $\xi$  space and there is no energy deviation among them. Approximate the amplitude  $|a|$  of the fundamental mode, the bunching parameter, is fixed for  $\tau = 0 \rightarrow 1$ . From the FEL pendulum equation

$$\frac{d\nu}{d\tau} = |a| \cos(\xi + \phi) \quad (11)$$

we can see how the initial uniformly distributed electrons in  $\xi$  (from  $-\pi$  to  $\pi$ ) evolve in  $\xi$  space as time proceeds. This bunching mechanism through Eqn.(11) is due to the interaction between the electrons and the fundamental mode and does not consider further bunching due to the other harmonics in this paper. Fig.3 demonstrates the electron density of a microbunch,  $N_m(\xi, \tau)$ , based on Eqn.(11) with  $|a| = 1.19, \nu_0 = 2.6$ [11] and  $\phi = 0$ , where  $|a|$  corresponds to about one percent of the

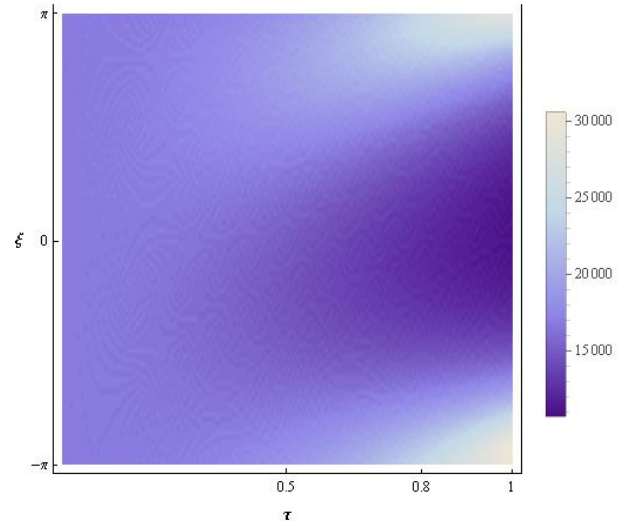


FIG. 3.  $N_m(\xi, \tau)$ .

FEL saturation. Ignore the coulomb force, which will be small, as shown in [12]. Impose the condition of electron number for each microbunch within a micropulse,  $n_m = \frac{I}{ce} \lambda_1 \simeq 1.675 \times 10^6$ , on  $N_m(\xi, \tau)$  which can be

decomposed as

$$N_m(\xi, \tau) = \sum_{k=-\infty}^{\infty} \tilde{N}_k(\tau) e^{k\xi i} \quad (12)$$

As the width  $\Delta\xi$  of the peak in Fig.3 is  $\Delta\xi \simeq \frac{\pi}{4}$  at  $\tau \simeq 1$ , different  $\phi$  in Eqn.(11) would not alter  $|\tilde{N}_7|$  much, considering the period  $\frac{2\pi}{7}$  of  $e^{7\xi i}$ . Fig.4 is  $N_7(\tau) = |\tilde{N}_7|$ . As the beam proceeds, it forms the  $\tilde{N}_7$  approaching  $\tau = 1$ , as shown in Fig.4. Name the time period between  $\tau = 0.92$  and  $\tau = 1$  with the large  $\tilde{N}_7$  as 7th zone.

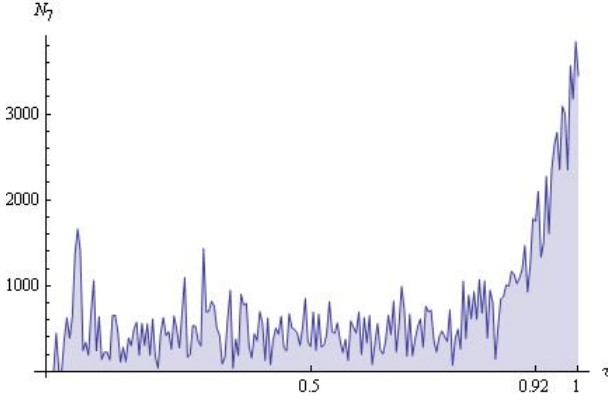


FIG. 4.  $N_7(\tau) = |\tilde{N}_7|$ .

From now on, assume that the microbunches only within the 7th zone contribute to the integration of Eqn.(10). Each electron in the 7th zone corresponding to the same  $\xi_p$  has a different  $\zeta_{p_n}$  and  $\rho_{p_n}$ . In the 7th zone, the range of  $\rho$  is  $0 \leq \rho \leq 1$ , and  $\zeta$ 's range is  $\frac{0.42L_w}{z_R} \simeq 22.7 < \zeta < \frac{0.5L_w}{z_R} \simeq 27.0$ . Therefore, approximate  $e^{-\frac{\rho_{p_n}^2}{1+\zeta_{p_n}^2}}$  and  $e^{-\frac{\zeta_{p_n}\rho_{p_n}^2 i}{1+\zeta_{p_n}^2}}$  to 1, and  $e^{tan^{-1}(\zeta_{p_n})i}$  to i. And as  $N_7$  is highly peaked at  $\tau = 1$ , apply  $\zeta_{p_n} \simeq 27.0$  in Eqn.(10). From now on, treat each micropulse as a point particle as each micropulse's length  $l_m = t_m c = 6 \times 10^{-4}[m]$  is much shorter than the spacing between each of the micropulses,  $l_s = \frac{c}{f_m} \simeq 0.105[m]$  and  $l_7 = 0.08L_w$ , the length of the 7th zone. Then, with  $b = \sqrt{\frac{2}{1+27.0^2}} \simeq 0.052$ , and considering that there is only one micropulse at most in the 7th zone as  $l_s > l_7$ , obtain

$$c_0^7(t) = -b \frac{J_0 J J_7}{\epsilon_0 V_{opt7}} \alpha N p i \tilde{N}_{7avg} t \quad (13)$$

where  $\alpha = 0.07$  is the ratio of the cross section of the 7th harmonic to that of the electron beam, and  $N = \frac{l_m}{\lambda_1} \simeq 2.24 \times 10^2$  is the number of microbunches in a micropulse, with  $t_7 = \frac{l_7}{c}$  and  $p = \frac{l_7}{l_s} \simeq 8.23 \times 10^{-1}$ , the fraction of time when a micropulse is present within the 7th zone.

And the  $|\tilde{N}_{7avg}|$  is

$$|\tilde{N}_{7avg}| = \left| \frac{1}{t_7} \int_{t_7} \sum_{p=1}^{N_{phase}} N_m(\xi_p, t') e^{-7\xi_p i} dt' \right| \quad (14)$$

$$\simeq 2.531 \times 10^3$$

Then, according to Eqn.(6), G becomes

$$G = \left| b \frac{J_0 J J_7}{\epsilon_0 V_{opt7}} \alpha N p \tilde{N}_{7avg} t \right|^2 \frac{V_{opt7} \epsilon_0}{\hbar \omega_7} = g_0 t^2 \quad (15)$$

where

$$g_0 = \frac{|b J_0 J J_7 \alpha N p \tilde{N}_{7avg}|^2}{\epsilon_0 V_{opt7} \hbar \omega_7} \simeq 7.25 \times 10^{15} [s^{-2}] \quad (16)$$

However, the cavity loss for one cavity round trip,  $C_R$ , has not been considered. Taking that into consideration, G becomes

$$G = 4g_0 \left( \frac{t_R (1 - e^{-\frac{C_R}{2t_R} t})}{C_R} \right)^2 \quad (17)$$

*Quantum current operator J and the mechanism of radiation.*—From Maxwell's equation,

$$\nabla^2 B(r, t) - \frac{1}{c^2} \frac{\partial^2}{\partial t^2} B(r, t) = -\mu_0 \nabla \times J(r, t) \quad (18)$$

we can see that when the electromagnetic field is quantized, the current density  $J$  is also a quantum operator; Eqn.(18)'s left hand side is a second order differential equation and its right hand side is a first order differentiation, so quantum J is proportional to quantum B which is periodic, and J contains the quanta of photon. Then, as the  $B$  field has two quantum quadratures  $X_1$  and  $X_2$ ,  $J$  has the observables in phase with  $X_1$  or  $X_2$ . Because  $\Delta\xi \simeq \frac{\pi}{4}$  is the width for the electron density's peak in the 7th zone as shown in Fig.3 and  $\Delta\Phi = \frac{\pi}{2}$  is the phase difference for Eqn.(2) and Eqn.(3), we can assume all the electrons in the 7th zone are classically in phase with the  $X_2$ , considering the microbunching optimized for the amplification of the 7th harmonic field, i.e. microbunch's transverse velocity in the 7th zone is in phase with the co-propagating electric field.

Let the position of the microbunch treated as a point particle, because  $l_m$  is much smaller than  $\lambda_w$ , be at  $z = Z$ . Name the observable, in phase with  $X_2$  at  $z = Z$ , A (Here, we can find the justification of setting  $X_1$  and  $X_2$  as the two observables among the possible choice of phases for the two observables). For the J's observable in phase with  $X_1$  or  $-X_1$ , we can think of the two observables nearest from A, located at  $z = Z + \frac{\lambda_w}{4}$  and  $z = Z - \frac{\lambda_w}{4}$  as the phase difference of  $\Delta\Phi = \frac{\pi}{2}$  corresponds to  $\frac{\pi}{2} \frac{\lambda_w}{2\pi} = \frac{\lambda_w}{4}$  difference in z space. Name the first one B and the second one  $B'$ . From Eqn.(2), A's transverse velocity,  $\dot{x}_A$ , satisfies  $\dot{x}_A \propto -\cos(\frac{2\pi}{\lambda_w} z) \propto \vec{E}$

where  $\vec{E}$  is the co-propagating field from Eqn.(1), i.e. A's transverse velocity is in phase with the co-propagating electric field. Then B satisfies  $\dot{x}_B \propto \sin(\frac{2\pi}{\lambda_w}z)$  and  $\ddot{x}_B \propto \cos(\frac{2\pi}{\lambda_w}z)$ . Therefore, B's radiated field satisfies  $\vec{E}_{rad,B} \propto q\ddot{x}_B \propto -\cos(\frac{2\pi}{\lambda_w}z)$ , meaning  $\vec{E}_{rad,B}$  is in phase with the co-propagating electric field. Therefore, B cannot amplify but can radiate. For  $B'$ , it satisfies  $\dot{x}_{B'} \propto -\sin(\frac{2\pi}{\lambda_w}z)$  and  $\ddot{x}_{B'} \propto -\cos(\frac{2\pi}{\lambda_w}z)$ . Therefore,  $\vec{E}_{rad,B'} \propto q\ddot{x}_{B'} \propto \cos(\frac{2\pi}{\lambda_w}z)$ , meaning  $\vec{E}_{rad,B'}$  is not in phase with the co-propagating electric field. Therefore,  $B'$  can neither amplify nor radiate, so we can ignore the observable  $B'$ . Now, we can see the quantum J should be decomposed into two observables A and B, which are point particles that are assumed to be negative charges like the electrons. Although the microbunch is classically in phase with the  $X_2$ , because of the nonzero quantum vacuum field, this decomposition is available as shown in Fig.5.

In the mechanism of a micropulse's radiation, A is in charge of the amplification while B is in charge of the radiation regarding to the co-propagating electric field, i.e. the energy source of B's radiation is the A's lost energy. This simultaneous cooperation between A and B although there is spatial distance of  $\frac{\lambda_w}{4}$  between them, which is originated from the quantum entanglement between the two observables of J operator, is the Radiation Mechanism. In the Radiation Mechanism, as A cannot radiate, the microbunch's radiation can be possible solely by B. And as the radiation field is in phase with  $\ddot{x}$  according to the Lienard Wiechert potential, only if B can radiate, assume all the energy transferred from the microbunch to the field increases  $|\alpha|$  while leaving  $\sinh^2(r)$  unchanged in Eqn.(6). Here, we can see the Radiation Mechanism is available only when both A and B are oscillating within the wiggler.

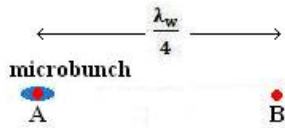


FIG. 5. Decomposition of J of a micropulse into the two observables.

*Squeezing Mechanism.*—When a micropulse is oscillating at the last section with length of  $\frac{\lambda_w}{4}$  in the 7th zone, named as the squeezing zone shown in Fig.6, we cannot have the observable B, as there can be no further oscillation outside the wiggler. Therefore, there is only amplification due to A without the simultaneously accompanying radiation by B. To satisfy the instantaneous energy conservation for a micropulse within the squeezing zone, the energy lost from the micropulse via A should be transferred to the 7th harmonic not by the increase of  $|\alpha|$ , the Radiation Mechanism, but rather by squeezing the vacuum fluctuations through  $\sinh^2(r)$  in Eqn.(6) by

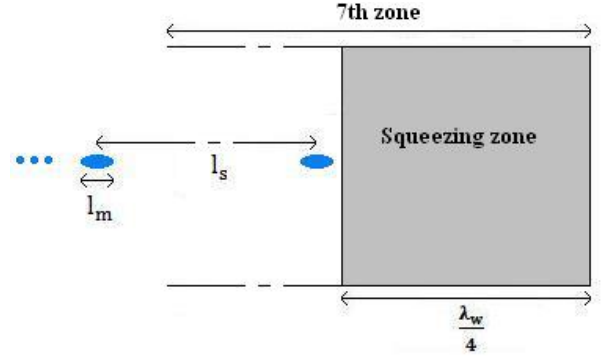


FIG. 6. The squeezing zone inside the 7th zone.

amplifying  $X_2$ . This is the Squeezing Mechanism mentioned above.

Considering the  $2\pi$  period of  $\sin$ , it could be claimed that another observable in phase with the  $X_1$  named as  $B''$  also can exist at  $z = Z - \frac{3}{4}\lambda_w$ . However, as the micropulse is localized, we can approximately ignore  $B''$ , and it is similar for A; only the nearest two observables from the micropulse, A and B, are of consideration.

*Comparison between data and calculation.*—From Eqn.(17), the G for  $t = t_s \simeq 80ns$ , the sampling time period, is  $G \simeq 19.4$ . At the end of  $t_s$ , the excited number of the detector's atoms, the counted photon number, will be close to  $G$ [13]. Considering  $\eta_e = 0.1176$ , the net system quantum efficiency, and  $t_s$ , the calculated photon count rate  $R_p$  becomes the following.

$$R_p = \frac{\eta_e G}{t_s} \simeq 2.85 \times 10^7 [s^{-1}] \quad (19)$$

which is about three percent above the range of the measured one, between  $2.275 \times 10^7 [s^{-1}]$  and  $2.773 \times 10^7 [s^{-1}]$ .

	Data	Calculation
Photon count	$(2.275 \sim 2.773) \times 10^7 [s^{-1}]$	$2.85 \times 10^7 [s^{-1}]$
Fano factor	0.22 ~ 0.44	0.41

TABLE I. Comparison between data[2] and calculation.

The  $G_s$  due to the Squeezing Mechanism during  $t_s$  can be obtained from Eqn.(17) with the modification of  $p = \frac{\lambda_w}{l_s} \simeq 5.47 \times 10^{-2}$  and  $|\tilde{N}_{avg}| \simeq 4000$  considering the maximum of  $N_7$  in Fig.4. Then  $G_s$  becomes approximately 0.214, corresponding to  $F \simeq 0.41$  from Eqn.(7), which is consistent with the data,  $F \simeq 0.22 \sim 0.44$ [3].

During  $t_s$ , the detector accumulates the photon number and the Fano factor of  $F \simeq 0.41$  is for the photons at  $t \simeq t_s$ . However, photons detected earlier than  $t = t_s$  possess larger F, so the accumulated photon's F can be

Parameters	Value	Unit
$\lambda_w$ =Wiggler period	2.3	cm
$N_w$ =Number of wiggler periods	47	
$L_w = N_w \lambda_w$ =Length of the wiggler	1.081	m
Wiggler gap	60~62	mm
$L_c$ =Cavity length	2.046	m
$z_R$ =Raleigh length for 7th harmonic	2.0	cm
$C_R$ =Cavity loss for 7th harmonic	0.323	
Transmission at 7th harmonic	25%	
Macropulse length	2	$\mu s$
$f_M$ =Macropulse repetition rate	15	Hz
$t_m$ =Micropulse length	2	ps
$f_m$ =Micropulse repetition rate	2.856	GHz
$E_b$ =Average beam energy	43.5	Mev
Energy spread(FWHM)	0.4%	
I=Peak micropulse current	30	A
Average micropulse current	171.4	mA
$\lambda_1$ =Fundamental mode wavelength	2.68	$\mu m$
Macropulse length	1.7	$\mu s$
Micropulse length	2	ps
Spectral width(FWHM)	0.5 %	
$\lambda_7$ =7th harmonic wavelength	382	nm
$k_7 = \frac{2\pi}{\lambda_7}$	$1.64 \times 10^7$	$m^{-1}$
$w_{07} = \sqrt{\frac{2z_R}{k_7}}$	$4.93 \times 10^{-5}$	m
$V_{opt7} = \pi w_{07}^2 L_c$	$1.56 \times 10^{-8}$	$m^3$
$t_R$ =Cavity round trip time	13.6555	ns
FEL round trip gain	145.63%	
$\gamma = \frac{\omega_7}{m_e c^2} - 1$	$4.93 \times 10^{15}$	Hz
$K = \frac{e B_0 \lambda_w}{2\pi m_e c} = \text{Undulator parameter}$	1.13	
$t_r$ =Sampling period	80	ns
$\eta_e$ =Net system quantum efficiency	11.76%	

TABLE II. Operation parameters of MARKIII FEL[14].

larger than 0.41, but as  $G \propto t^2$  in Eqn.(15), the F's deviation from 0.41 would be small if the count was done periodically at a constant period. If there is an asymmetry in the rate of heat loss for  $|\alpha|^2$  and  $\sinh^2(r)$ , it can affect the F calculated, which has not been considered in this paper.

*Conclusions.*—Chen's discovery of the sub-Poisson photon number distribution of the FEL is from the squeezed vacuum fluctuations due to the quantum current at the right edge of the wiggler. Simultaneous communication between A and B across nonzero spatial distance because of quantum entanglement, which enables

the electromagnetic radiation, seems to be related to the Wheeler Feynman's absorber theory[15] that explains the instantaneous radiation reaction force or the Fluctuation Dissipation Theorem that can instantaneously relate the boundary condition with the FEL's vacuum fluctuations[6].

The author wishes to acknowledge John M. J. Madey for the initial ideas, discussion and invaluable inspiration.

---

\* jwpark@hawaii.edu

- [1] W. Becker, M. O. Scully, and M.S. Zubairy, "Generation of squeezed coherent states via a free-electron laser", Phys. Rev. Lett. **48**, 475 (1982).
- [2] Teng Chen and John M. J. Madey, "Observation of sub-Poisson fluctuations in the intensity of the seventh coherent spontaneous harmonic emitted by a rf linac free-electron laser", Phys. Rev. Lett. **86**, 5906 (2001).
- [3] Teng Chen and John M. J. Madey, "Effects of Electron Shot Noise and Quantum Field Fluctuations on the Photon Statistics of the Coherent Spontaneous Harmonic Radiation", IEEE J. Quantum Electron. **44**, 294 (2008).
- [4] John M. J. Madey, "Wilson Prize article: From vacuum tubes to lasers and back again", Phys. Rev. ST Accel. Beams **17**, 074901-14 (2014).
- [5] Roy J. Glauber, *Quantum Theory of Optical Coherence*, 1st edition (WILEY-VCH, 2007), p. 5.
- [6] John M. J. Madey, private communication.
- [7] Hans-A. Bachor and Timothy C. Ralph, *A guide to Experiments in Quantum Optics*, 2nd revised and enlarged edition (Wiley-VCH, 2004), pp. 238-241.
- [8] Hans-A. Bachor and Timothy C. Ralph, [7], p. 242.
- [9] L. H. Yu *et al.*, "First ultraviolet high-gain harmonic-generation free-electron laser", Phys. Rev. Lett. **91**, 074801 (2003).
- [10] Peter Schmüser, Martin Dohlus, Jörg Rossbach, Christopher Behrens, *Free-Electron Lasers in the Ultraviolet and X-Ray Regime*, Second Edition (Springer, 2014), p. 25.
- [11] Eric B. Szarmes, *Classical Theory of Free-Electron Lasers*, 1st edition (Morgan & Claypool, 2014), p. 51.
- [12] W. B. Colson, "The nonlinear wave equation for higher harmonics in free-electron lasers", IEEE J. Quantum Electron. QE-17, 1417 (1981).
- [13] Roy J. Glauber, [5], pp. 459-460.
- [14] Teng Chen, "Photon statistics of coherent harmonic radiation of a linac free electron laser", Ph.D. thesis, Duke University, 1999.
- [15] J. Wheeler and R. Feynman, "Interaction with the absorber as the mechanism of radiation", Rev. Mod. Phys. **17**, 157 (1945).